Muñoz-Moreno, L. et al. (2018) 'Growth hormone-releasing hormone receptor antagonists modify molecular machinery in the progression of prostate cancer', The Prostate, 78(12), pp. 915–926.

Growth hormone-releasing hormone receptor antagonists modify molecular machinery in the progression of prostate cancer

Laura Muñoz-Moreno[1], Andrew V. Schally[2,3], Juan C. Prieto[1], M. José Carmena[1], Ana M. Bajo[1,*]

[1] *Department of Systems Biology, University of Alcalá, Alcalá de Henares, Madrid, Spain*

[2] *Veterans Affairs Medical Center, Miami, Florida*

[3] *Departments of Pathology and Medicine, Divisions of Hematology/Oncology, Sylvester Comprehensive Cancer Center, University of Miami, Miller School of Medicine, Miami, Florida*

* Corresponding author. Address: Department of Systems Biology, University of Alcalá, 28871 Alcalá de Henares, Spain. Tel.: +34-91-885-5114. E-mail address: ana.bajo@uah.es (A.M. Bajo).

Abstract

Background: Therapeutic strategies should be designed to transform aggressive prostate cancer phenotypes to a chronic situation. To evaluate the effects of the new growth hormone-releasing hormone receptor (GHRH-R) antagonists: MIA-602, MIA-606, and MIA-690 on processes associated with cancer progression as cell proliferation, adhesion, migration, and angiogenesis.

Methods: We used three human prostate cell lines (RWPE-1, LNCaP, and PC3). We analyzed several molecules such as E-cadherin, β-catenin, Bcl2, Bax, p53, MMP2, MMP9, PCNA, and VEGF and signaling mechanisms that are involved on effects exerted by GHRH-R antagonists.

Results: GHRH-R antagonists decreased cell viability and provoked a reduction in proliferation in LNCaP and PC3 cells. Moreover, GHRH-R antagonists caused a time-dependent increase of cell adhesion in all three cell lines and retarded the wound closure with the highest value with MIA-690 in PC3 cells. GHRH-R antagonists also provoked a large number of cells in SubG0 phase revealing an increase in apoptotic cells in PC3 cell line.

Conclusions: Taken all together, GHRH-R antagonists of the MIAMI series appear to be inhibitors of tumor progression in prostate cancer and should be considered for use in future therapeutic strategies on this malignancy.

Keywords: antagonists, angiogenesis, cell adhesion, cell proliferation, GHRH-R, prostate cancer.

1. Introduction

One in nine men over the age of 65 will develop invasive prostate cancer (PC). Prostate cancer is the most common non-cutaneous cancer in men and an international health problem.[1] The prognosis of PC varies greatly, being highly dependent on factors such as stage of diagnosis, race, and age. Treatment of PC includes prostatectomy, androgen deprivation, and radiation. However, metastatic prostate cancer usually acquires resistance to androgen deprivation therapy and current treatments are only palliative. In this regard, bone metastases, with an incidence of 85% in patients with advanced stages of the disease, is the most common cause of death.[2] Therapeutic strategies should be designed to transform aggressive prostate cancer phenotypes to a chronic situation.[3]

Growth hormone-releasing hormone (GHRH) is a neuropeptide secreted by the hypothalamus and, after binding to GHRH receptors in the pituitary gland (pGHRHR), stimulates the synthesis and release of GH. GH in turn induces the production of the insulin-like growth factor I, a known mitogen in many cell types, associated with malignant transformation, tumor progression and metastasis of various cancers.[4] The expression of GHRH and its receptors has been detected in normal cells and many human tumor.[5–8] In recent years, the group of one of us (AVS) has synthesized numerous GHRH-R antagonists that act directly on tumor cells inhibiting proliferation in vitro and in vivo.[9,10] The combination of these analogues with cytotoxic compounds can potentiate inhibition of tumor growth.[11]

The routes of intracellular signal transduction involved in the antiproliferative effects of GHRH-R antagonists have not been fully identified. Intracellular second messengers involved in signaling path- ways of GHRH-R analogs mediated by tumoral GHRH-R such as cAMP and Ca^{2+} activate specific isoforms of PKC, MAPK, PKA, Src, ADAMs, and the oncogenes c-fos and c-jun.[12–14] GHRH-R antagonists of the recent MIA series such as MIA-602, MIA-606, MIA-690

show a high binding affinity to the pituitary type of GHRH receptors on tumors and their splice variant and exert potent inhibitory effects on various tumors including gastric cancer, pancreatic, and ovarian cancer at very low doses.

Uncontrolled proliferation can be linked to a reduced apoptosis which promotes tumor progression.[15] Both, apoptosis and proliferation processes, are connected by cell-cycle regulators. Molecules such us the proliferating cell nuclear antigen (PCNA), p53, p21, and anti- and pro-apoptotic proteins, can be deregulated, provoking an unbalancing of proliferation and death cell.[16–20] On the other hand, cell adhesion is an essential capability for growth, migration, and differentiation in human cells.[21–23] Cellular adhesion molecules (CAMs) play a pivotal role in the development of invasive and distant metastasis.[24] E-cadherin is a member of CAM family, which mediates cell-cell contact and acts as an important suppressor of tumor cell invasiveness and metastasis. E-cadherin and β-catenin are involved in signal transduction mechanisms that regulate cell growth, migration, and differentiation.[25–28] The release of β-catenin in the perinuclear region is associated with the transcription factor Lef/TCF (Lymphoid enhancer factor/T cell factor). The resulting complex is translocated into the nucleus to activate target gene transcription associated with tumor progression such as cyclin D1, CD44, c-myc, metalloproteinases (MMP), and vascular endothelial cell growth factor (VEGF).[29]

In this study, we used three human prostate cell lines to evaluate the effects of the GHRH-R antagonists of the MIA series: MIA-602, MIA-606, and MIA-690 on cell proliferation, adhesion, migration, and angiogenesis, typically associated with cancer progression. Several other molecules and signaling mechanisms, which are involved in effects exerted by GHRH-R antagonists, were also analyzed.

2. Materials and methods

2.1. Peptides

GHRH-R antagonists of the MIA series, MIA-602, MIA-606, and MIA-690 were synthesized by solid phase methods in the laboratories of one of us (AVS).[30]

2.2. Cell culture

Three human prostate cell lines were used. Non-neoplastic, immortalized adult human prostatic epithelial cells (RWPE-1) are androgen-responsive and show many normal cell characteristics. The two human prostate cancer cell lines used exhibit different features of prostate cancer progression from early stages to androgen independence stages. LNCaP is an androgen-responsive cancer cell line and PC3 is an androgen- unresponsive cell line that may be related to recurrent prostate cancers that have achieved androgen independence. Cell lines were obtained from the American Type Culture Collection. RWPE-1 cells were maintained in complete keratinocyte serum-free medium (K-SFM) containing bovine pituitary extract (50 μg/mL) and epidermal growth factor (5 ng/mL). LNCaP and PC3 cells were grown and maintained in RPMI-1640 medium supplemented with 10% fetal bovine serum (FBS, Invitrogen, Barcelona, Spain). All culture media were also supplemented with 1% penicillin/ streptomycin/amphotericin B (Life Technologies, Carlsbad, CA). The culture was performed in a humidified 5% CO_2 environment at 37°C. After the cells reached 70-80% confluence, they were washed with PBS, detached with 0.25% trypsin/0.2% EDTA, and seeded at 30 000-40 000 cells/cm^2. The culture medium was changed every 3 days.

2.3. Cell viability studies

Cells were grown to 70-80% confluence, harvested with trypsin/EDTA solution and seeded at low concentration (50 000 cells per well) in 24-well plates for 24 h. The culture medium was then

removed and replaced with RPMI-1640 medium containing 1% antibiotic/antimycotic (penicillin/streptomycin/amphotericin B) and 0% FBS for 24 h. Cells were treated for 24 h with 0.1 μM GHRH-R antagonists. Cell viability was determined by tetrazolium assay, which measures the reduction of substrate MTT [3-(4,5-dimethylthiazol-2-yl)2,5-diphenyltetrazolium bromide] to a dark blue formazan product by mitochondrial dehydrogenases in living cells. MTT (5 mg/mL) (Sigma–Aldrich, Alcobendas, Madrid, Spain) was added to each well and the mixture incubated for 3 h at 37°C in darkness. The medium was replaced and the dark blue formazan precipitate was dissolved with 0.2 N HCl in isopropanol. Absorbance was read at 570 nm in a plate reader (ELX 800, Bio-Tek Instruments, Winooski, VT). Results were expressed as the relative percentage of absorbance compared with control cells.

2.4. Cell proliferation assays

RWPE-1, LNCaP, and PC3 (2×10^5) cells were grown in six-well plates. After 24 h, the culture medium was removed and replaced with RPMI-1640 medium containing 0% FBS and 1% antibiotic/antimycotic (penicillin/streptomycin/amphotericin B) for 16 h. Then, cells were subjected for 24 h to different treatments. In the last 30 min of incubation, cells were pulsed with 10 μM bromodeoxyuridine (BrdU). Thereafter, cells were washed with PBS, fixed with ice-cold absolute ethanol, and stored at −20°C for 30 min. Fixative was removed by centrifugation and the cell pellets were washed with PBS. DNA was partially denatured by incubation with 1 M HCl for 30 min at room temperature and then the cells were washed three times with PBS containing 0.05% Tween-20 (pH 7.4) and 0.1% BSA. Cells were incubated with 20 μl of anti-BrdU monoclonal antibody with FITC (BD Bioscience, San Agustin de Guadalix, Spain) in the dark for another 30 min period. In preparation for flow cytometry analysis, the cells were stained with propidium iodide (PI) staining solution: PI (50 μg/mL) and RNase (10 μg/mL) in PBS. The

number of BrdU-positive cells was counted with the use of the Cyflogic program (Version 1.2.1.).

2.5. Cell cycle assays

PC-3 (2×10^5) cells were grown in six-well plates. After 24 h, the culture medium was removed and replaced with RPMI-1640 medium containing 0% FBS and 1% antibiotic/antimycotic (penicillin/ streptomycin/amphotericin B) for 16 h. After that, cells were subjected to the various treatments for 6 h. Then the cells were washed with PBS and detached with 0.25% trypsin/0.2% EDTA. The cells were centrifuged at 500 xg for 5 min at 4°C and the pellets were mixed with ice-cold 70% ethanol and then kept at −20°C for 30 min. After removing the ethanol by centrifugation, the pellets were washed with PBS and centrifuged again. The supernatants were discarded and the pellets suspended in PBS, 0.2 mg/mL RNase A and 20 µg/mL PI before flow cytometry analysis with a FACSCalibur cytometer (Becton Dickinson, San Agustin de Guadalix, Spain). Results obtained were analyzed with the Cyflogic v 1.2.1 program.

2.6. Cell adhesion assay

Concentrated type-I collagen solution was diluted in 10 mM glacial acetic acid and coated onto 96-well plates for 1 h at 37°C. Plates were washed twice with PBS (pH 7.4). Cells were harvested with 0.25% trypsin/0.2% EDTA and collected by centrifugation. They were resuspended in RPMI medium/0.1% (w/v) BSA (pH 7.4) and treated with 0.1 µM GHRH(1-29)NH2 for 30 min. Then, cells plated at 2.5×10^4 cells per 100 µl. The assay was terminated at indicated time intervals (0-80 min) by aspiration of the wells. Cell adhesion was quantified by adding MTT (1 mg/mL) followed by 1 h incubation. Isopropanol (50 µl) was added to each well to dissolve the formazan precipitates and absorbance at 540 nm with a reference wavelength at 630 nm was reported.

2.7. Wound-healing assay

RWPE-1 and PC3 cells were incubated in 24-well plates and a small wound area was made in the confluent monolayer with a scraper. Afterward, cells were incubated in the absence or presence of MIA-602, MIA-606, and MIA-690 (0.1 μM). Four representative fields of each wound were captured using a Nikon Diaphot 300 inverted microscopy at different times (0-24 h). Wound areas of untreated samples were averaged and assigned a value of 100%.

2.8. Cell lysates isolation

RWPE-1, LNCaP, and PC3 cells (1.5–3× 10^6 cells) were washed with ice-cold PBS and then harvested, scraped into ice-cold PBS, and pelleted by centrifugation at 500 xg for 5 min at 4°C. For preparation of cell lysates, cells were kept on ice for 30 min in a solution containing 20 mM Tris-HCl (pH 7.5), 1 mM EDTA, 0.5 M NaCl, 1 mM EDTA, 2 mM PMSF, 5 μg/mL aprotinin, 5 μg/mL leupeptin, 5 μg/mL pepstatin. Thereafter, cells were pelleted by centrifugation at 4 000 xg for 5 min at 4°C.

2.9. Western blot assays

Proteins from cell lysates (30 μg) extracts were denatured by heating. Then, they were resolved by 10% SDS-PAGE, and blotted onto a nitrocellulose membrane (BioTrace/NT, Quimigen, Madrid, Spain) overnight in 50 mM Tris-HCl, 380 mM glycin, 0.1% SDS, and 20% methanol. Anti-E-cadherin (BD Biosciences Cat# 610181, RRID: AB_397580) and anti-β-catenin (BD Biosciences Cat# 610154, RRID: AB_397555), anti-Bcl2 (Santa Cruz Biotechnology, Santa Cruz, CA, Cat# sc-509, RRID: AB_626733) and anti-Bax (Santa Cruz Biotechnology Cat# sc-493, RRID: AB_2227995), anti-p53 (Sigma–Aldrich Cat# sc-126, RRID: AB_628082), anti-MMP2 (Abcam, Cambridge, UK, Cat# ab52756, RRID: AB_880701) and anti-MMP9 (Abcam Cat# ab76003,

RRID: AB_1310463), and anti-PCNA (Innovative Research, Le-Perray-en-Yvelines, France, Cat# 18-0110, RRID: AB_86659) antibodies were added followed by incubation for 1 h at room temperature. After treatment for 1 h at room temperature with the corresponding secondary antiserum (1:4,000 for anti-rabbit serum and for anti-mouse serum), the signals were detected with enhanced chemiluminescence reagent (Pierce, Rockford, IL) using β-actin antibody as loading control.

2.10. RNA isolation and RT-PCR

PC3 cells were placed in six-well plates (15×10^4 cells) and incubated with the different treatments in serum medium for different periods of time. Total RNA was isolated with Tri-Reagent (Sigma–Aldrich) according to the instructions of the manufacturer. Two microgram of total RNA were reverse-transcribed using 6 μg of hexamer random primer and 200 U M-MLV RT (Life Technologies) in the buffer supplied with the enzyme, supplemented with 1.6 μg/mL oligo dT, 10 nM dithiothreitol (DTT), 40 U RNasin (Promega, Madison, WI), and 0.5 mM deoxyribonucleotides (dNTPs). Two microliter of the RT reaction were used for each PCR amplification, with a primer set which amplifies cDNAs for human cysteine rich protein with CD44, Cyclin D1, c-Myc, MMP9 y MMP2, or β-actin. The corresponding sequences of oligonucleotide primers were as follows in Table 1. PCR-conditions were: denaturation at 94°C for 5 min, followed by 26-40 cycles of 95°C for 1 min, 57°C for 1 min, 72°C for 1 min, and then a final cycle of 10 min at 72°C. The signals were normalized with the β-actin gene expression level. The PCR products were separated by electrophoresis and visualized in 2% agarose gels, stained with GelRedTM nucleic acid gel stain (Biotium, Hayward, CA) and visualized under ultraviolet light.

2.11. Determination of VEGF

VEGF levels in tumor homogenates (15 μg) were determined by using the human VEGF DuoSet (R&D Systems, Minneapolis, MN) according to the manufacturer's instructions. Data were normalized by the protein concentration in each sample.

2.12. Gelatin zymography

Zimography assays were carried out as described previously.[31] Briefly, the samples (30 μg of protein) were subjected to 10% SDS-PAGE with 0.1% (w/v) gelatin (Sigma–Aldrich) as the substrate. After staining, the activity of MMP2 and MMP9 was semiquantitatively determined by densitometry.

2.13. Data analysis

Quantification of band densities was performed using Quantitive One Program (Bio-Rad, Alcobendas, Spain). Data were subjected to one-way ANOVA and differences were determined by Bonferroni's multiple comparison test. Each experiment was repeated at least three times. Data are shown as the means of individual experiments and presented as the mean ± SEM. $P < 0.05$ was considered statistically significant.

3. Results

3.1. Effect of GHRH-R antagonists on cell viability and proliferation in RWPE-1, LNCaP, and PC3 cells

The effect of GHRH-R antagonists, 0.1 μM MIA-602, MIA-606, and MIA-690 on the cell viability and proliferation of RWPE-1, LNCaP, and PC3 cells were assessed by MTT and BrdU incorporation assays, respectively (Figures 1A and 1B). Incubation of cells with 0.1 μM GHRH-R antagonists significantly decreased ($P < 0.001$) cell viability (27-44% vs control).

The treatment with GHRH-R antagonists showed a different behavior on the proliferation of each cell line (Figure 1B). In RWPE-1 cells, only MIA-602 antagonist caused a 42% reduction ($P < 0.01$) on cell proliferation. However, all antagonists studied provoked a reduction in proliferation in LNCaP and PC3 cells. Interestingly, GHRH-R antagonist MIA-690 caused a significant decrease ($P < 0.001$) of up to 40-50% compared to its control value.

To determine whether GHRH-R antagonists modified the expression of the molecule involved on cell proliferation, PCNA, we treated the three cell lines with MIA-602, MIA-606, and MIA-690. Treatment with GHRH-R antagonists significantly reduced PCNA expression in both RWPE-1 cells (MIA-606 and MIA-690, up to 36 and 22%, respectively) and in LNCaP cells (MIA-602 and MIA-690, up to 24 and 39%, respectively) (Figure 1C). In PC3 cells, all of the antagonists of the MIA series caused significant changes ($P < 0.001$) in PCNA expression levels, where the biggest decline was reached after treatment with MIA-690 (49%).

3.2. Effect of GHRH-R antagonists on cell cycle in PC3 cells

This procedure to analyze cell cycle is based in cellular DNA content. It reveals distribution of cells in three major phases of the cycle and makes possible to detect apoptotic cells with fractional DNA content. Thus SubGo phase determines whether DNA has been damaged and the genetic material is hypodiploid (< 2n). PC3 cells were treated for 8 h with 0.1 μM GHRH-R antagonists. After treatment with GHRH-R antagonists, there was a large number of cells in SubG0 phase revealing an increase in apoptotic cells (Figure 2A). Moreover, GHRH-R antagonists caused a very notorious increase of cells in S-phase as well as a corresponding decrease of those in the G1 and G2/M phases which induced S-phase arrest.

Changes in cell cycle by GHRH-R antagonists may be due to variations on the expression of molecules involved in cell cycle. Therefore, the levels of p53, p21, Bax, and Bcl2 were analyzed

after appropriate treatment in PC3 cells. GHRH-R antagonists significantly increased ($P < 0.01$) both p53 mRNA and protein expression at 30 and 45 min, respectively (Figures 2B and 2C). Furthermore, after 2 h-treatment with MIA-690 antagonist mRNA levels for p21 were significantly increased by 50% ($P < 0.001$) (Figure 2D). On the other hand, treatment with GHRH-R antagonists (Figure 2E) provoked a decrease in expression of Bcl2 and increased Bax levels, resulting in augmenting of the Bax/Bcl2 ratio value, which indicates a rise in cell apoptosis.

3.3. Effect of GHRH-R antagonists on cell adhesion in RWPE-1, LNCaP, and PC3 cells

The effects of GHRH-R antagonists (MIA-602, MIA-606, and MIA-690) on cell adhesion of RWPE-1, LNCaP, and PC3 cells were assessed by assays of collagen adhesion. Cells were suspended and incubated for 30 min with 1 μM GHRH-R antagonists. Then, cells were placed in 96-well plates with collagen and removed at different times (Figure 3A). Thereafter, the cells were incubated with MTT and measured by cell adhesion assay. The results show that treatment with GHRH-R antagonists caused a time-dependent significant increase ($P < 0.001$) of cell adhesion in all three cell lines, with the highest value with MIA-690 at 80 min in PC3 cells (83%).

In order to know whether variations of cell adhesion caused by GHRH-R antagonists affected to adhesion molecules, we evaluated E-cadherin protein levels after treatment with 0.1 μM GHRH-R antagonists for 8 h by Western blot analysis. The results show that E-cadherin protein levels were significantly increased ($P < 0.01$- $P < 0.001$) in prostate cancer cell lines being higher with MIA-690. However, no changes were observed in RWPE-1 cells (Figure 3B).

3.4. Effect of GHRH-R antagonists on the expression levels of β-catenin.

In addition to their adhesive functions, the E-cadherin/β-catenin complex also plays a key role in modulating Wnt signaling, both processes involved in cancer progression. E-cadherin/β-catenin complex maintains integrity of epithelial cell-cell contact and keeps Wnt/β-catenin signals in

check. Levels of β-catenin were analyzed by Western blotting after treatment with MIA antagonists in LNCaP and PC3 cells since both showed changes in E-cadherin expression (Figure 4A). Expression levels of β-catenin were significantly reduced at 8 h in the presence of GHRH-R antagonists. PC3 cells show a greater reduction (44-48%) as compared to that in LNCaP cells (17-20%). These effects were correlated with the increase produced in E-cadherin by GHRH-R antagonists.

Subcellular distribution of β-catenin is important in the Wnt signaling pathway. Therefore, we assessed its expression in cytosols and nuclei after treatment with GHRH-R antagonists MIA-602, MIA-606, and MIA-690. For this purpose, the PC3 cell line was selected since it was where a further decrease in the expression of β-catenin occurred after treatment with GHRH-R antagonists. The expression of cytosolic β-catenin significantly increased and the nuclear expression decreased, after 2 h of treatment with GHRH-R antagonists (Figure 4B).

The increase of β-catenin protein levels in the nucleus of PC3 cells could induce transcription of target genes such as CD44, c-myc, and cyclin D1. Therefore, mRNA levels of these genes were analyzed by RT-PCR assays after treatment with 0.1 μM GHRH-R antagonists in PC3 cells (Figure 4C). GHRH-R antagonists significantly reduced mRNA levels of the three target genes. MIA-690 antagonist was the most effective because it provoked a decline of the three genes by 52-78% as compared with control values.

3.5. Effect of GHRH-R antagonists on cell migration in RWPE-1 and PC3 cells

Cancer cells begin to migrate to other tissues after the loss of cell adhesion. We evaluated by means of wound-healing assay the migratory capability of RWPE-1 and PC3 cells after treatment with GHRH-R antagonists (MIA-602, MIA-606, and MIA-690). Results show that GHRH-R antagonists retarded the wound closure in both cells lines (Figure 5). The greatest retardation effect

was observed in PC3 cells after the treatment with GHRH-R antagonists (Figure 5B).

In order to analyze the molecules involved in migration process, we assessed mRNA levels and gelatinolytic activity of metalloproteinases 2 and 9 (MMP2 and MMP9) at 45 min and 2 h, respectively. Levels of mRNA of both metalloproteases were decreased at 45 min after treatment with GHRH-R antagonists (Figure 6A). Antagonist MIA-690 was the most effective agent since mRNA levels of MMPs were significantly reduced by 60% ($P < 0.001$). The gelatinolytic activity (Figure 6B) of both pro-MMP2 and −9 was reduced after 2 h of treatment with antagonists. MIA-690 caused the greatest reduction in both pro-MMPs (by 78% for pro-MMP2 and 54% for pro-MMP9).

3.6. Effect of GHRH-R antagonists on VEGF secretion in PC3 cells

VEGF is the main pro-angiogenic factors involved in tumor progression and it is related to molecules involved in migration and adhesion as β-catenin or MMP9. Levels of VEGF125 released by the cells to the extracellular medium after 24 h-treatment with GHRH-R antagonists were assessed by ELISA. VEGF protein levels were decreased by 31% after treatment with GHRH-R antagonists as compared to those in the control (Figure 6C).

4. Discussion

Currently, PC is the most frequent non-cutaneous cancer among men and the second leading cause of cancer related deaths. Various reports have demonstrated the anti-tumor activity of GHRH-R antagonists against several cancer types.[5,8–14] In the current study, we investigated the effect of three GHRH-R antagonists, MIA-602, MIA-606, and MIA-690, in human non-tumoral prostate cells and in prostate tumors on processes associated with cancer progression.

In our study, GHRH-R antagonists MIA-606 and MIA-690 reduced proliferation only in two tumor lines, but MIA-602 decreased proliferation of three cell lines studied. Similar inhibition has

been described by the group of one of us (AVS).[11,30,32] In this regard, the lower-proliferation induced by GHRH-R antagonists of the MIA series was accompanied by a reduction on PCNA levels. This fact could decrease the processivity of DNA polymerase blocking the initiation cell replication. In this regard, a previous antagonist JMR-132, from which the MIA series proceeded, reduced the expression of PCNA in human benign prostatic hyperplasia cells.[33] Our results show that GHRH-R antagonists of the latest MIA series increased apoptotic cells and arrested cell cycle in S phase in more aggressive prostate cancer cell line, which could explain that both cell viability and proliferation decreased. Similar effects of JMR-132 were reported in colon cancer cells.[32] These antagonists provoke DNA damage, which mediates cell cycle arrest and apoptosis through the activation of p53, p21, and Bax, as well as the suppression of the antiapoptotic protein Bcl-2.[34] Present results indicate that the effects of GHRH-R antagonists on the cell cycle could be due to both a decrease of p21, p53, and Bax and a rise of Bcl-2. Consequently, the increased ratio of proapoptotic/antiapoptotic molecules may activate the process of programmed cell death.

Epithelial-to-mesenchymal transition represents one major mechanism in cancer cell metastasis.[28] Epithelial molecule E-cadherin regulates cell-to-cell contact and its aberrant or decreased expression is considered as one of the biomarkers for poor prognosis in PC.[35] These facts support the relevance of the increased E-cadherin protein levels induced by GHRH-R antagonists of the MIA series in prostate cancer cells. Similar results have been described in breast cancer cells after treatment with MIA-602 antagonist.[36] In epithelial cells, E-cadherin-β- catenin association prevents the release of β-catenin to the cytoplasm and subsequent translocation to the nucleus, where it activates the transcription of genes that promote tumor progression.[37] In our study, GHRH-R antagonists reduced β-catenin levels in the nucleus. Comparable outcomes have been obtained in glioblastoma cells, breast cancer, and ovarian cancer in the presence of the antagonist MIA-602.[36]

The lower presence of nuclear β-catenin would prevent the activation of transcription of target genes, c-myc, cyclin D1, and CD44 as was observed in our in vitro experiments. The importance of GRHR-R antagonists on the reduction of c-myc, cyclin D1, and CD44 Levels lies in the capability of such molecules to prevent cell cycle progression, reduce cell adhesion, and increase tumor proliferation.[38–40]

When tumor cells lose their adherence ability, they are able to migrate to other tissues. In this process, degradation of the extracellular matrix is produced by proteolytic enzymes, mainly MMP9 and MMP2, which are highly expressed in prostate tumor tissue in advanced stage.[41] Our results indicate that GHRH-R antagonists reduced both cell motility in the prostate and MMPs levels in prostate cancer cells. This fact would block steps of the metastatic process, preventing the invasion of blood vessels, and colonization of other tissues. Similar results have been described by dealing with MIA-602 cells from breast cancer, ovarian cancer, and glioblastoma.[36] In addition, GHRH-R antagonists reduced levels of the major pro-angiogenic molecule, VEGF, by stablishing an anti-angiogenic role for the novel MIA-series antagonists. The effects of MZ-J-7-118 and RC-3940-II antagonists in advanced PC cells have been described validating the current results.[42] Moreover, it has been found that under hypoxic conditions, such as inside tumor mass, an increase occurs of MMP2 and 9, and in turn upregulates VEGF levels.[41,43]

Conclusion

In conclusion, GHRH-R antagonists of the MIA series could be defined as inhibitors of tumor progression in prostate cancer and should be considered for use in future therapeutic strategies.

Acknowledgments

This study was supported by a grant from the Junta de Comunidades de Castilla-La Mancha (PII10-0189-3222 to A.M.B) and the Universidad de Alcalá (CCG2015/BIO-010 to A.M.B.).

Conflicts of interest

None of the authors has any conflicts of interest regarding this study.

Funding information

Junta de Comunidades de Castilla-La Mancha, Grant number: PII10-0189-3222; Universidad de Alcalá (Spain), Grant number: CCG2015/ BIO-010

References

1. Siegel RL, Miller KD, Jemal A. Cancer statistics, 2016. *CA Cancer J Clin.* 2016;66: 7–30.

2. Sottnik JL, Dai J, Zhang H, Campbell B, Keller ET. Tumor-induced pressure in the bone microenvironment causes osteocytes to promote the growth of prostate cancer bone metastases. *Cancer Res*. 2015;75: 2151–2158.

3. Lage A, Crombet T. Control of advanced cancer: the road to chronicity. *Int J Environ Res Public Health*. 2011;8: 683–697.

4. Schally AV, Varga JL, Engel JB. Antagonists of growth-hormone- releasing hormone: an emerging new therapy for cancer. *Nat Clin Pract Endocrinol Metab.* 2008;4: 33–43.

5. Busto R, Schally AV, Varga JL, et al. The expression of growth hormone-releasing hormone (GHRH) and splice variants of its receptor in human gastroenteropancreatic carcinomas. *Proc Natl Acad Sci U S A*. 2002;99: 11866–11871.

6. Halmos G, Schally AV, Czompoly T, Krupa M, Varga JL, Rekasi Z. Expression of growth hormone-releasing hormone and its receptor splice variants in human prostate cancer. *J Clin Endocrinol Metab*. 2002;87: 4707–4714.

7. Havt A, Schally AV, Halmos G, et al. The expression of the pituitary growth hormone-releasing hormone receptor and its splice variants in normal and neoplastic human tissues. *Proc Natl Acad Sci U S A*. 2005;102: 17424–17429.

8. Kahán Z, Arencibia JM, Csernus VJ, et al. Expression of growth hormone-releasing hormone (GHRH) messenger ribonucleic acid and the presence of biologically active GHRH in human breast, endome- trial, and ovarian cancers. *J Clin Endocrinol Metab*. 1999;84: 582–589.

9. Stangelberger A, Schally AV, Djavan B. New treatment approaches for prostate cancer based on peptide analogues. *Eur Urol*. 2008;53: 890–900.

10. Muñoz-Moreno L, Arenas MI, Schally AV, et al. Inhibitory effects of antagonists of growth hormone-releasing hormone on growth and invasiveness of PC3 human prostate cancer. *Int J Cancer* 2013;132: 755–765.

11. Buchholz S, Schally AV, Engel JB, et al. Potentiation of mammary cancer inhibition by combination of antagonists of growth hormone- releasing hormone with docetaxel. *Proc Natl Acad Sci U S A*. 2007;104: 1943–1946.

12. Garcia-Fernandez MO, Schally AV, Varga JL, Groot K, Busto R. The expression of growth hormone-releasing hormone (GHRH) and its receptor splice variants in human breast cancer lines; the evaluation of signaling mechanisms in the stimulation of cell proliferation. Breast Cancer Res Treat. 2003;77: 15–26.

13. Kanashiro CA, Schally AV, Zarandi M, Hammann BD, Varga JL. Suppression of growth of H-69 small cell lung carcinoma by antagonists of growth hormone releasing hormone and bombesin is associated with an inhibition of protein kinase C signaling. *Int J Cancer*. 2004;112: 570–576.

14. Munoz-Moreno L, Arenas MI, Carmena MJ, Schally AV, Prieto JC, Bajo AM. Growth hormone-releasing hormone antagonists abolish the transactivation of human epidermal growth factor receptors in advanced prostate cancer models. *Invest New Drugs.* 2014;32: 871–882.

15. Kirby RS, Partin AW, Feneley M, Parsons JK. *Prostate Cancer: Principles and Practice*.

London and New York: Taylor & Francis; 2006.

16. Moldovan GL, Pfander B, Jentsch S. PCNA, the maestro of the replication fork. *Cell*. 2007;129: 665–679.

17. Waga S, Stillman B. Cyclin-dependent kinase inhibitor p21 modulates the DNA primer-template recognition complex. *Mol Cell Biol.* 1998;18: 4177–4187.

18. Abbas T, Dutta A. P21 in cancer: intricate networks and multiple activities. *Nat Rev Cancer*. 2009;9: 400–414.

19. Pérez-Sayáns M, Suárez-Peñaranda JM, Gayoso-Diz P, Barros- Angueira F, Gándara-Rey JM, García-García A. The role of p21Waf1/CIP1 as a Cip/Kip type cell-cycle regulator in oral squamous cell carcinoma (Review). *Med Oral Patol Oral Cir Bucal.* 2013;18: e219–e225.

20. Mirzayans R, Andrais B, Scott A, Murray D. New insights into p53 signaling and cancer cell response to DNA damage: implications for cancer therapy. *J Biomed Biotechnol.* 2012;2012:170325.

21. Gumbiner BM. Cell Adhesion: The Molecular Basis of Tissue Architecture and Morphogenesis. *Cell*. 1996;84: 345–357.

22. Cavallaro U. Cell adhesion and signalling by cadherins and Ig-CAMs in cancer. *Nat Rev Cancer*. 2004;4: 118–132.

23. Hanahan D, Weinberg Robert A. Hallmarks of Cancer: The Next Generation. *Cell*. 2011;144: 646–674.

24. Drivalos A, Papatsoris AG, Chrisofos M, Efstathiou E, Dimopoulos MA. The role of the cell adhesion molecules (integrins/cadherins) in prostate cancer. *Int Braz J Urol.* 2011;37: 302–306.

25. Mărgineanu E, Cotrutz CE, Cotrutz C. Correlation between E-cadherin abnormal expressions in different types of cancer and the process of metastasis. *Rev Med Chir Soc Med Nat Iasi.*

2008;112: 432–436.

26. Beuran M, Negoi I, Paun S, et al. The epithelial to mesenchymal transition in pancreatic cancer: A systematic review. *Pancreatology*. 2015;15: 217–225.

27. Le Bras GF, Taubenslag KJ, Andl CD. The regulation of cell-cell adhesion during epithelial-mesenchymal transition, motility and tumor progression. *Cell Adh Migr.* 2012;6: 365–373.

28. Onder TT, Gupta PB, Mani SA, Yang J, Lander ES, Weinberg RA. Loss of E-cadherin promotes metastasis via multiple downstream tran- scriptional pathways. *Cancer Res.* 2008;68: 3645–3654.

29. Thakur R, Mishra DP. Pharmacological modulation of beta-catenin and its applications in cancer therapy. *J Cell Mol Med*. 2013;17: 449–456.

30. Zarandi M, Varga JL, Schally AV, et al. Lipopeptide antagonists of growth hormone-releasing hormone with improved antitumor activi- ties. *Proc Natl Acad Sci U S A*. 2006;103: 4610–4615.

31. Fernández-Martínez AB, Bajo AM, Sánchez-Chapado M, Prieto JC, Carmena MJ. Vasoactive intestinal peptide behaves as a pro-metastatic factor in human prostate cancer cells. *Prostate*. 2009;69: 774–786.

32. Rick FG, Schally AV, Szalontay L, et al. Antagonists of growth hormone-releasing hormone inhibit growth of androgen-independent prostate cancer through inactivation of ERK and Akt kinases. *Proc Natl Acad Sci U S A*. 2012;109: 1655–1660.

33. Siejka A, Schally AV, Block NL, Barabutis N. Antagonists of growth hormone-releasing hormone inhibit the proliferation of human benign prostatic hyperplasia cells. *Prostate*. 2010;70: 1087–1093.

34. Hohla F, Buchholz S, Schally AV, et al. GHRH antagonist causes DNA damage leading to p21 mediated cell cycle arrest and apoptosis in human colon cancer cells. *Cell Cycle*. 2009;8:

3149–3156.

35. Deep G, Gangar SC, Agarwal C, Agarwal R. Role of E-cadherin in antimigratory and antiinvasive efficacy of silibinin in prostate cancer cells. *Cancer Prev Res (Phila)*. 2011;4: 1222–1232.

36. Bellyei S, Schally AV, Zarandi M, Varga JL, Vidaurre I, Pozsgai E. GHRH antagonists reduce the invasive and metastatic potential of human cancer cell lines in vitro. *Cancer Lett*. 2010;293: 31–40.

37. Orsulic S, Huber O, Aberle H, Arnold S, Kemler R. E-cadherin binding prevents beta-catenin nuclear localization and beta-catenin/LEF-1- mediated transactivation. *J Cell Sci.* 1999;112: 1237–1245.

38. van de Wetering M, Sancho E, Verweij C, et al. The beta-catenin/TCF- 4 complex imposes a crypt progenitor phenotype on colorectal cancer cells. *Cell.* 2002;111: 241–250.

39. Chang G, Zhang H, Wang J, et al. CD44 targets Wnt/β-catenin pathway to mediate the proliferation of K562 cells. *Cancer Cell Int.* 2013;13: 117.

40. Ripple MJ, Parker Struckhoff A, Trillo-Tinoco J, et al. Activation of c-Myc and Cyclin D1 by JCV T-Antigen and β-Catenin in Colon Cancer. *PLoS ONE*. 2014;9: e106257.

41. Gong J, Zhu S, Zhang Y, Wang J. Interplay of VEGFa and MMP2 regulates invasion of glioblastoma. *Tumour Biol.* 2014;35: 11879–11885.

42. Stangelberger A, Schally AV, Varga JL, et al. Inhibition of human androgen-independent PC-3 and DU-145 prostate cancers by antagonists of bombesin and growth hormone releasing hormone is linked to PKC, MAPK and c-jun intracellular signalling. *Eur J Cancer.* 2005;41: 2735–2744.

43. Hollborn M, Stathopoulos C, Steffen A, Wiedemann P, Kohen L, Bringmann A. Positive

feedback regulation between MMP-9 and VEGF in human RPE cells. *Invest Ophthalmol Vis Sci.* 2007;48: 4360–4367.

Table 1. Oligonucleotide primers used in RT-PCR analysis for p53, p21, CD44, c-myc, cyclin D1, MMP9, MMP2, and β-actin expression in human prostate PC3 cells. Primers were chosen with the assistance of the computer program Primer Express (Perkin Elmer Applied Biosystems).

mRNA	Primer	Sequence (5'→ 3')
p53	sense	AGGCCTTGGAACTCAAGG
	antisense	TGAGTCAGGCCTTCTGTCT
p21	sense	AGGTGAGGGGACTCCAAAGT
	antisense	ATGAAATTCACCCCCTTTCC
CD44	sense	AAGGTGGAGCAAACACAACC
	antisense	ACTGCAATGCAAACTGCAAG
c-myc	sense	AGCGACTCTGAGGAGGAACA
	antisense	CTCTGACCTTTTGCCAGGAG
cyiclin D1	sense	TTCGGGATGATTGGAATAGC
	antisense	TGTGAGCTGGTTCATTGAG
MMP9	sense	TGGGCTACGTGACCTATGACA
	antisense	TGTGGCAGCACCAGGGCAGC
MMP2	sense	ACCTGGATGCCGTCGTGGAC
	antisense	TGTGGCAGCACCAGGGCAGC
β-actin	sense	AGAAGGATTCCTATGTGGGCG
	antisense	CATGTCGTCCCAGTTGGTGAC

Figure legends

Figure 1. Effect of 0.1 μM GHRH-R antagonists of the MIA series: MIA-602, MIA-606, and MIA-690 on cell viability (A), cell proliferation (B), and PCNA expression (C) assessed by MTT (A), BrdU incorporation (B) and Western blot (C) assays in RWPE-1, LNCaP, and PC3 cells. Results are expressed as percentage of control value. Data are mean ± SEM of 10 independent experiments; *, $P < 0.05$; **, $P < 0.01$; ***, $P < 0.001$.

Figure 2. Effect of 0.1 μM GHRH-R antagonists of the MIA series: MIA-602, MIA-606, and MIA-690 on cell cycle (A) and on expression levels of p53 (mRNA, B and protein, C), p21 (mRNA, D), and Bax/Bcl2 (protein, E) in PC3 cells. The study was performed by cell cycle (A), RT-PCR (B and D) and Western blot (C and E) assays. Results are expressed as percentage of control value. Data are mean ± SEM of four independent experiments; **, $P < 0.01$; ***, $P < 0.001$.

Figure 3. Effect of 0.1 μM GHRH-R antagonists, MIA-602, MIA-606, and MIA-690 on cell adhesion as assessed by collagen adhesion (A) and on the expression of E-cadherin as measured by Western blotting (B), in RWPE-1, LNCaP, and PC3 cell lines. Results are expressed as percentage relative to its corresponding control. Data are mean ± SEM of five independent experiments; **, $P < 0.01$; ***, $P < 0.001$.

Figure 4. Effect of 0.1 μM GHRH-R antagonists, MIA-602, MIA-606, and MIA-690 on the expression of β-catenin (A) in LNCaP and PC3 cells and on the location of β-catenin (B) and the expression of CD44, c-myc, and cyclin D1 (C) in PC3 cell line. The studies are performed using Western blot (A) and RT-PCR (B) assays. Results are expressed as a percentage relative to its corresponding control value. Data are mean ± SEM of three independent experiments; *, $P < 0.05$; **, $P < 0.01$; ***, $P < 0.001$.

Figure 5. Effect of 0.1 μM GHRH-R antagonists, MIA-602, MIA-606, and MIA-690 on cell migration in RWPE-1 (A) and PC3 (B) cells at different times (0-24 h) by means of wound-healing assays. Images are representatives of five independent experiments.

Figure 6. Effect of 0.1 μM GHRH-R antagonists, MIA-602, MIA-606, and MIA-690 on the expression of mRNA (A) and gelatinolitic activities of MMP9 and MMP2 (B), and the VEGF125 secretion (C) in PC3 cells. The studies are performed using RT-PCR (A), Western blot (B), and ELISA (C) assays. Results are expressed as a percentage relative to cells untreated. Data are mean ± SEM of three independent experiments; *, $P < 0.05$; **, $P < 0.01$; ***, $P < 0.001$, versus the corresponding control.

Figure 1

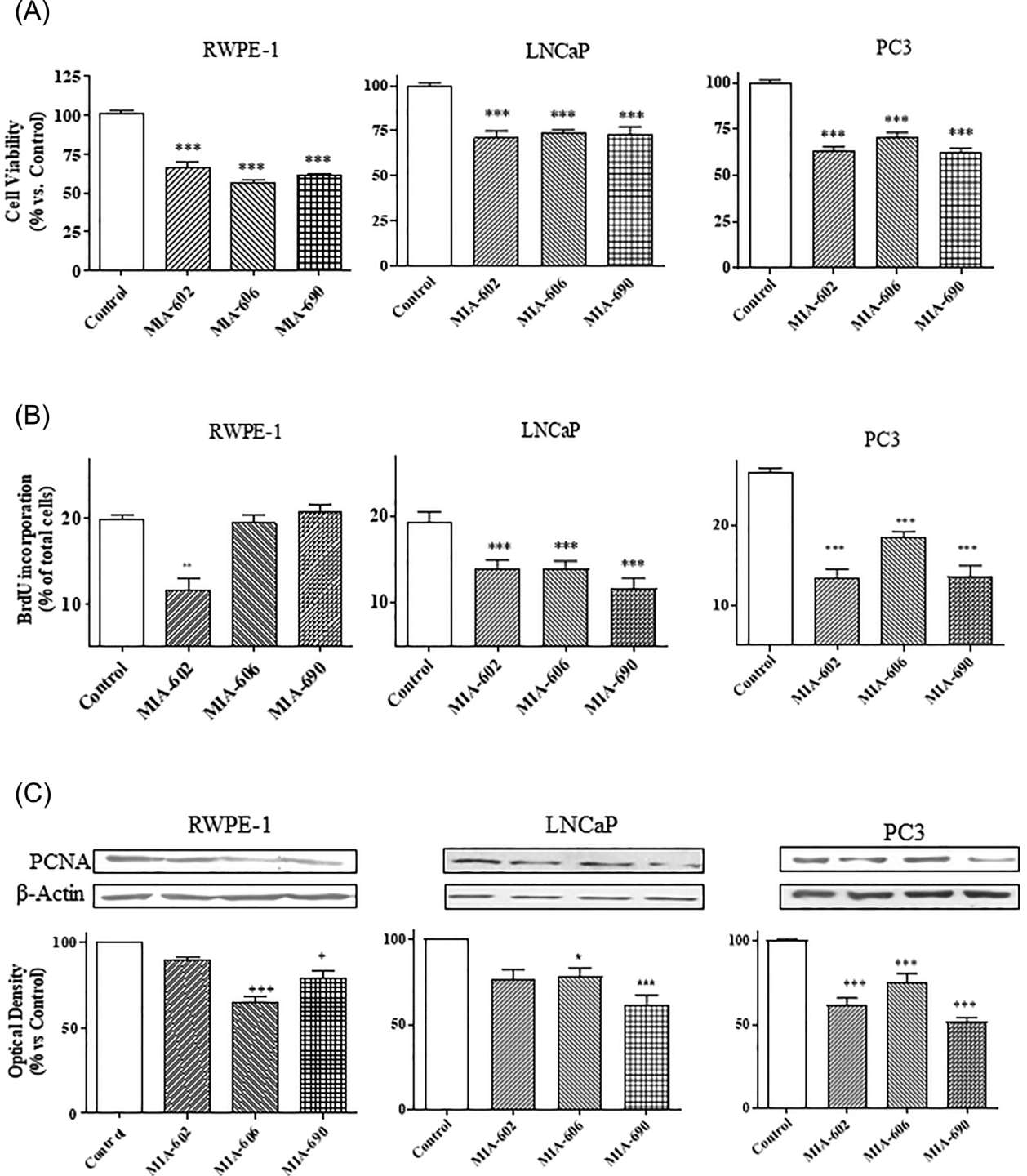
(A)
RWPE-1
LNCaP
PC3
Cell Viability (% vs. Control)
Control
MIA-602
MIA-606
MIA-690
(B)
RWPE-1
LNCaP
PC3
BrdU incorporation (% of total cells)
Control
MIA-602
MIA-606
MIA-690
(C)
RWPE-1
LNCaP
PC3
PCNA
β-Actin
Optical Density (% vs Control)
Control
MIA-602
MIA-606
MIA-690

Figure 2

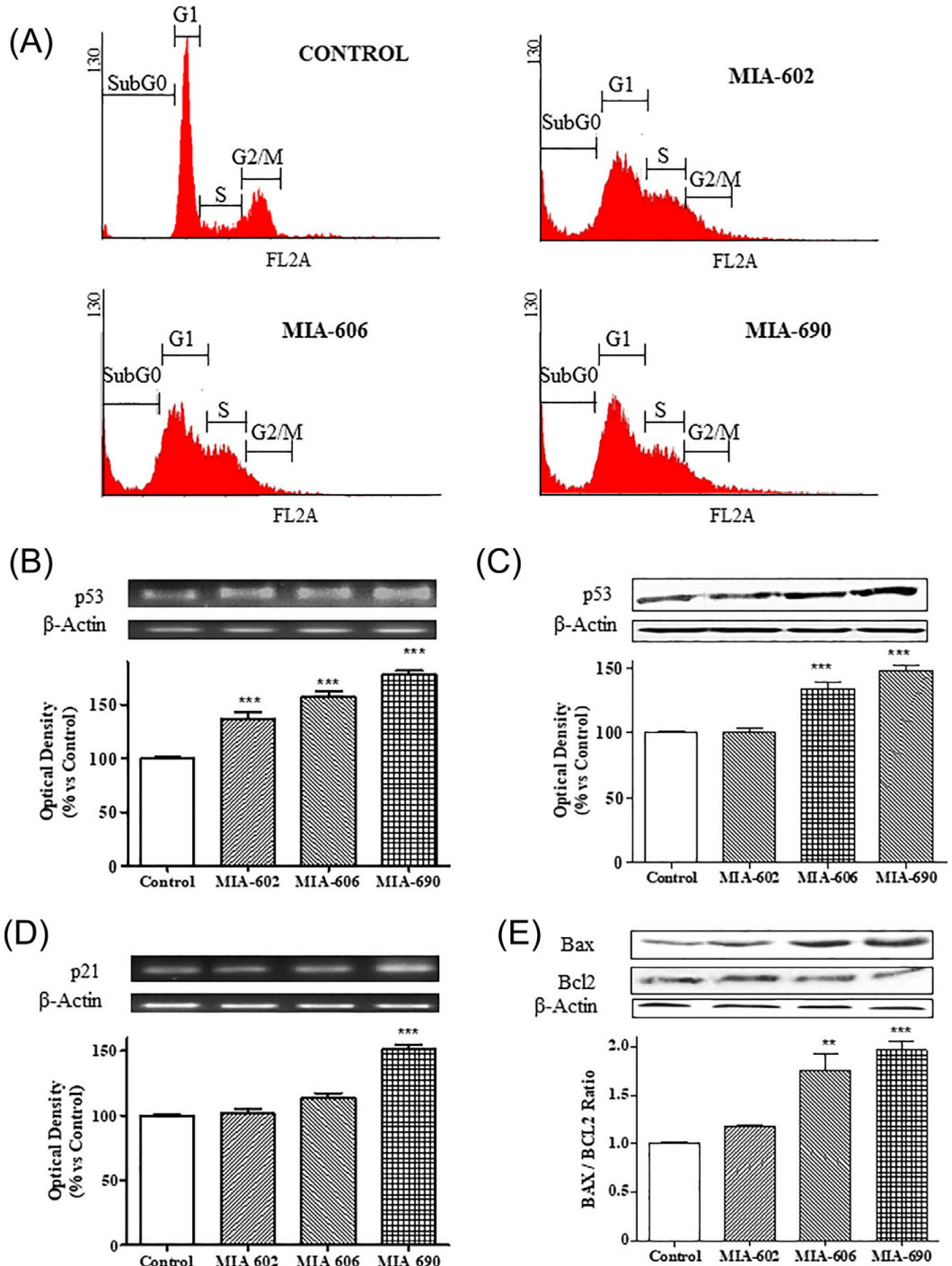
(A)
CONTROL
MIA-602
MIA-606
MIA-690
G1
SubG0
S
G2/M
130
FL2A
(B)
p53
β-Actin
Optical Density (% vs Control)
Control
MIA-602
MIA-606
MIA-690
(C)
p53
β-Actin
Optical Density (% vs Control)
(D)
p21
β-Actin
Optical Density (% vs Control)
(E)
Bax
Bcl2
β-Actin
BAX / BCL2 Ratio

Figure 3

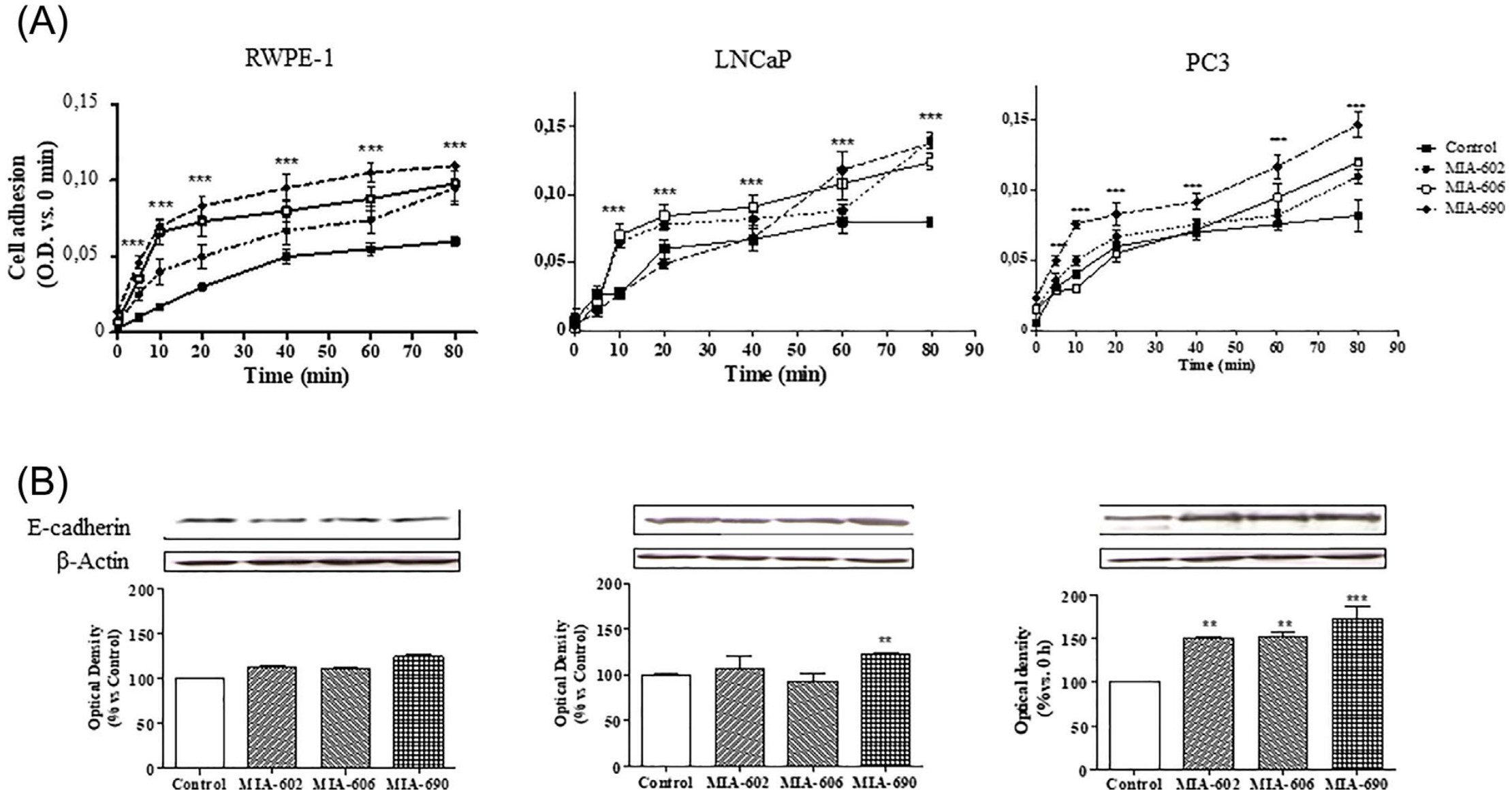
(A)
RWPE-1
LNCaP
PC3
Cell adhesion (O.D. vs. 0 min)
Time (min)
Control
MIA-602
MIA-606
MIA-690
(B)
E-cadherin
β-Actin
Optical Density (% vs Control)
Optical density (%vs. 0 h)
Control
MIA-602
MIA-606
MIA-690

Figure 4

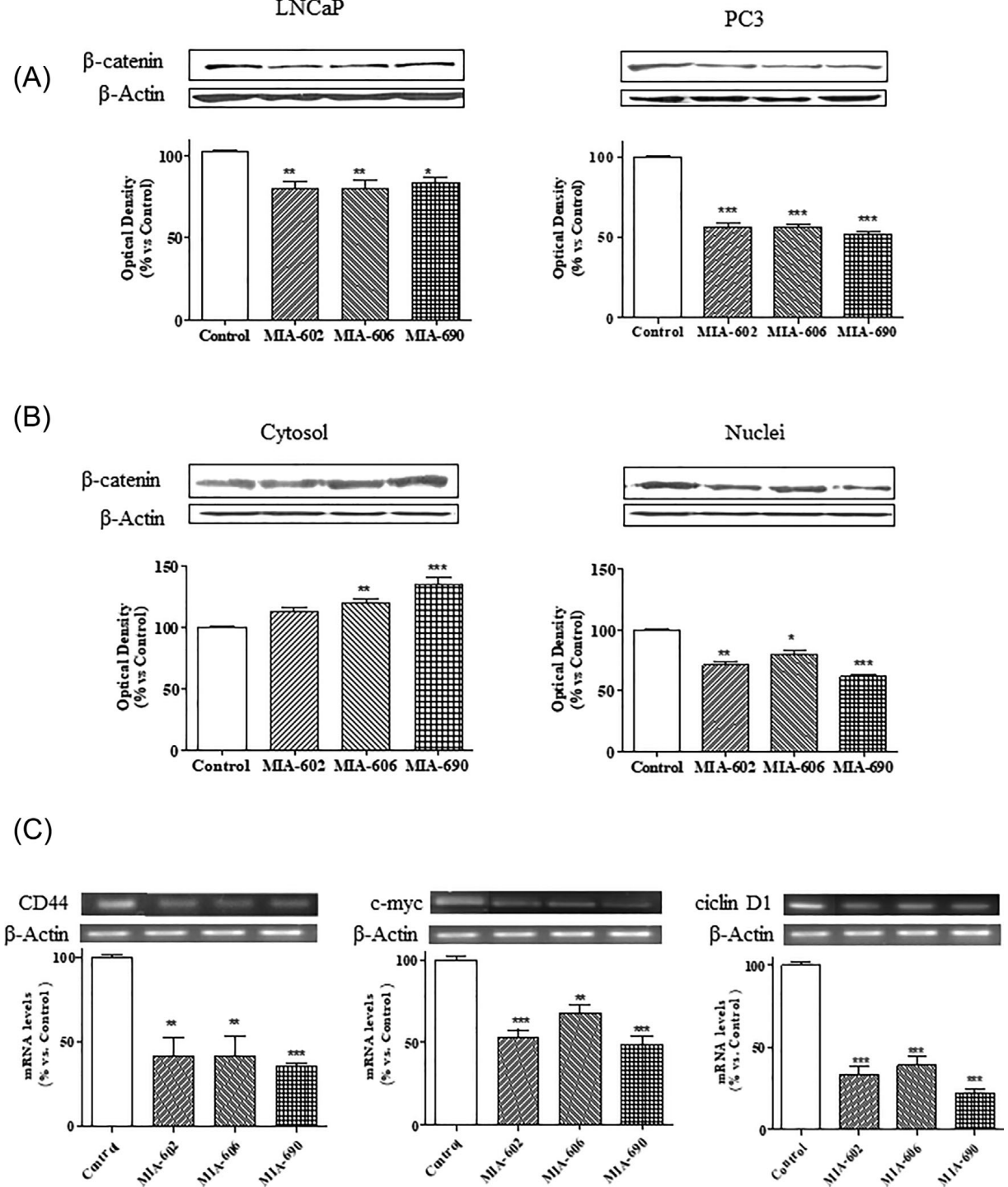
(A)
LNCaP
PC3
β-catenin
β-Actin
Optical Density (% vs Control)
Control
MIA-602
MIA-606
MIA-690
(B)
Cytosol
Nuclei
β-catenin
β-Actin
Optical Density (% vs Control)
Control
MIA-602
MIA-606
MIA-690
(C)
CD44
c-myc
ciclin D1
β-Actin
mRNA levels (% vs. Control)
Control
MIA-602
MIA-606
MIA-690

Figure 5

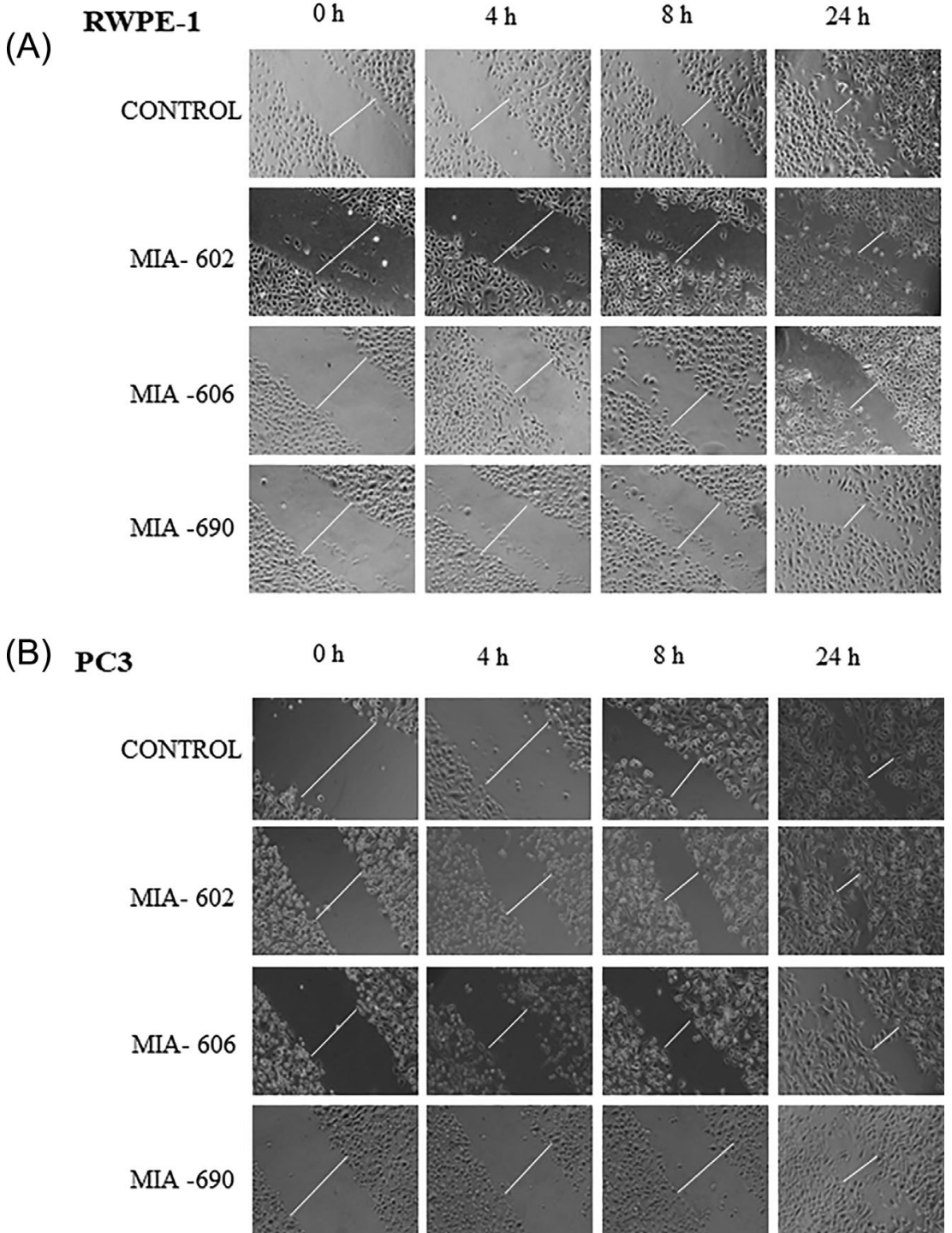
(A)
RWPE-1
0 h
4 h
8 h
24 h
CONTROL
MIA- 602
MIA -606
MIA -690
(B)
PC3
0 h
4 h
8 h
24 h
CONTROL
MIA- 602
MIA- 606
MIA -690

Figure 6

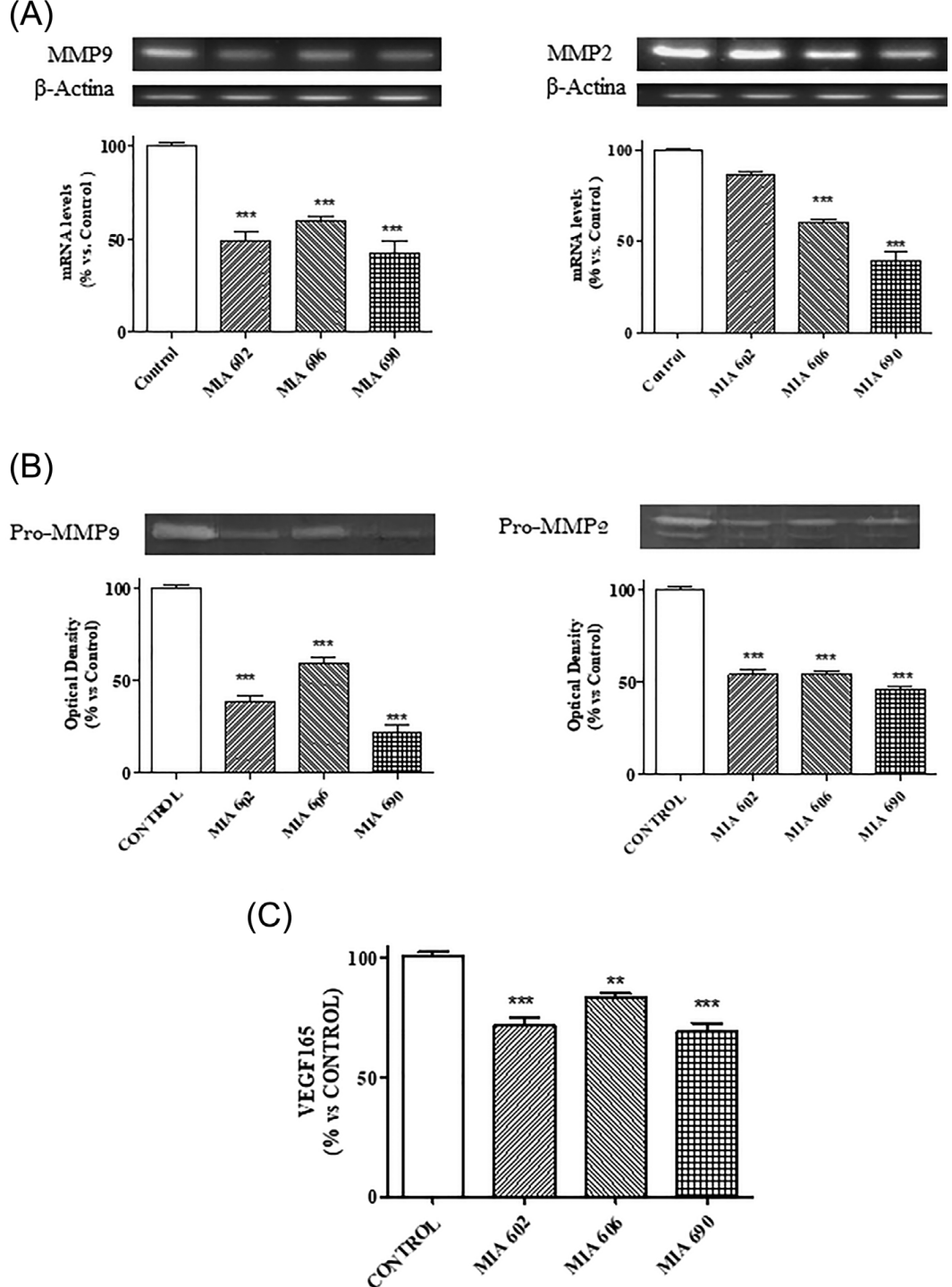
(A)
MMP9
β-Actina
MMP2
β-Actina
mRNA levels (% vs. Control)
100
50
0
***
Control
MIA 602
MIA 606
MIA 690
(B)
Pro-MMP9
Pro-MMP2
Optical Density (% vs Control)
CONTROL
(C)
VEGF165 (% vs CONTROL)
**